Dynamics of a Gas Bubble Moving in an Inviscid Liquid Subjected to a Sudden Pressure Change

Hsu-Chieh Yeh and Wen-Jei Yang

Department of Mechanical Engineering, The University of Michigan, Ann Arbor, Michigan 48104

(Received 10 June 1968; in final form 21 October 1968)

A gas bubble moves with constant translatory velocity in a quiescent liquid. Its shape deviates from sphericity due to asymmetrical forces exerted upon its surface. Then the liquid pressure undergoes a step change. It is the purpose of the study to analytically predict the time history of the bubble size, translatory velocity, and deformation. The mechanisms involved in the acceleration of the translatory motion and in the growth or collapse rate of the bubble are discussed.

INTRODUCTION

The translatory motion and deformation of a gas bubble moving in a source and/or sink flow have been investigated in Refs. 1 and 2. A brief review of the literature[3-7] concerned with the problems of the deformation and translatory motion of a gas bubble is presented in Ref. 2. From the study presented in Refs. 1 and 2, it is concluded that in a source and/or sink flow, the combined action of the translatory motion and the growth or collapse rate may cause the bubble to accelerate or decelerate its translatory motion. This conclusion has led to the conjecture that a gas bubble moving with a constant velocity in a quiescent liquid will be accelerated or decelerated as it grows or collapses following a change in the liquid pressure. With the motivation to prove the conjecture, work is undertaken in the present paper to analyze the time history of the velocity, size, and deformation of a gas bubble moving in a quiescent liquid whose pressure undergoes a step change in magnitude.

ANALYSIS

Consider a gas bubble traveling with velocity U in a quiescent liquid. The bubble deviates from spherical shape due to asymmetrical force exerted upon its surface. Then a step change in the pressure of the surrounding liquid is imposed on the system. For convenience in analysis, the coordinate systems (r, θ, ϕ) are fixed at the center of the moving bubble 0 in Fig. 1

with r measuring the radial distance, θ the angle between the radial vector, and the direction of the bubble velocity U. Let the instantaneous surface shape of the bubble be described by

$$r_s = R(t) + \sum_{n=1}^{\infty} a_n(t) P_n(\cos\theta), \qquad (1)$$
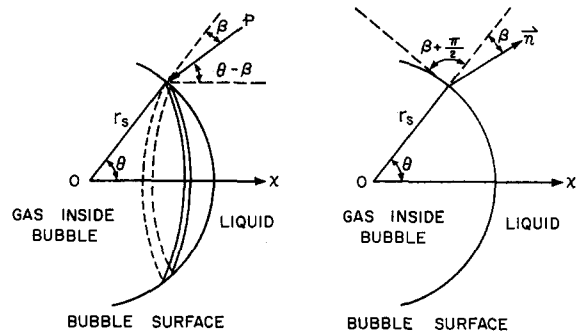

Fig. 1. Unit normal and pressure on a bubble surface.

where $R(t)$ is the radius of the unperturbed spherical bubble and all other terms describe the deviation from sphericity. $P_n(\cos\theta)$ are Legendre polynomials and a_n's are the time-dependent coefficients whose magnitudes are determined later in the Section.

The solution of the continuity equation for incompressible, irrotational fluid $\nabla^2\Phi = 0$ in moving coordinates is

$$\Phi = U\left(\frac{R^3}{2r^2} + r\right)\cos\theta + \frac{R^2\dot{R}}{r} + \sum_{n=1}^{\infty} \frac{C_n}{r^{n+1}} P_n(\cos\theta), \qquad (2)$$

where Φ is the velocity potential, the dot denotes the time derivative and C_n's are coefficients to be determined. When the coefficients C_n's are determined by the surface condition of the perturbed bubble, Eq. (2) may be re-

[1] H. C. Yeh, Ph.D. thesis, Mech. Engr. Dept., The University of Michigan (1967).
[2] H. C. Yeh, and W. J. Yang, J. Appl. Phys. **39**, 3156 (1968).
[3] M. S. Plesset and T. P. Mitchell, Quart. Appl. Math. **13**, 419 (1956).
[4] C. F. Naude, and A. T. Ellis, Trans. ASME, Ser. D J. Basis Engr. **83**, 648 (1961).
[5] R. A. Hartunian, and W. R. Sears, J. Fluid Mech. **3**, 27 (1957).
[6] J. K. Walters, and J. F. Davidson, Pt. 1, J. Fluid Mech. **12**, 408 (1962); Pt. 2, J. Fluid Mech. **17**, 321 (1963).
[7] R. D. Ivany, F. G. Hammitt, and T. M. Mitchell, Trans. ASME, Ser. D J. Basic Engr. **88**, 649 (1966).

written with the neglect of the terms involving a_n^2 as

$$\Phi = \frac{R^2\dot{R}}{r} - \sum_{n=1}^{\infty} (n+1)^{-1}\left(\dot{a}_n + 2\dot{R}\frac{a_n}{R}\right)\frac{R^{n+2}}{r^{n+1}}P_n + U\left[\left(r + \frac{R^3}{2r^2}\right)\cos\theta + \frac{3}{2}\sum_{n=1}^{\infty}a_n\left(\frac{n+1}{2n+1}\frac{R^{n+2}}{r^{n+2}}P_{n+1} - \frac{n-1}{2n+1}\frac{R^n}{r^n}P_{n-1}\right)\right],$$

(3)

in which recurrence formulas for $\sin^2\theta \cdot P_n'$ and $\cos\theta \cdot P_n^3$ have been used.

Now the r component of the equation of motion for an irrotational flow in an accelerating coordinate system in the absence of gravitational acceleration is integrated from r to infinity. With the aid of Eq. (3) and the recurrence formulas for $\sin^2\theta P_n'$, $\cos\theta P_n$ and $P_2 P_n$, it yields the expression for the liquid pressure distribution, from which the pressure distribution on the bubble surface may be obtained by replacing r by r_s as

$$\frac{p(r_s)}{\rho} = \frac{p_\infty}{\rho} + R\ddot{R} + \frac{3}{2}\dot{R}^2 - \frac{1}{4}U^2 - \frac{1}{2}Ua_1 - \frac{\dot{R}}{R}Ua_1 - \frac{1}{3}\dot{U}a_1 + \left\{\frac{1}{2}R\ddot{a}_1 + \frac{3}{2}\dot{R}\dot{a}_1 - \frac{9}{10}\frac{U^2}{R}a_1 - \frac{3}{10}\left[U\dot{a}_2 + \left(\dot{U} + 4U\frac{\dot{R}}{R}\right)a_2\right]\right.$$

$$+ \frac{27}{70}\frac{U^2}{R}a_3 + \frac{3}{2}\dot{R}U + \frac{1}{2}R\dot{U}\left.\right\}P_1 + \left\{\frac{3}{2}U\dot{a}_1 + \left(\frac{1}{3}\dot{U} + U\frac{\dot{R}}{R}\right)a_1 + \frac{1}{3}R\ddot{a}_2 + \dot{R}\dot{a}_2 - \left(\frac{1}{3}\ddot{R} + \frac{54}{35}\frac{U^2}{R}\right)a_2\right.$$

$$- \frac{3}{14}\left[5U\dot{a}_3 + \left(4\dot{U} + 6U\frac{\dot{R}}{R}\right)a_3\right] + \frac{U^2}{R}a_4 + \frac{3}{4}U^2\left.\right\}P_2 + \sum_{m=2}^{\infty}\left\{\frac{9}{4}\frac{m(m+1)(m+2)}{(2m+3)(2m+5)}\frac{U^2}{R}a_{m+2} - \frac{3}{2}\left[\frac{m+1.5(m+1)}{2m+3}\dot{U}a_{m+1}\right.\right.$$

$$+ \frac{(m+1)(m+4)}{2m+3}U\frac{\dot{R}}{R}a_{m+1} + \frac{2m+1}{2m+3}\ddot{R}a_m + \frac{9}{4}\frac{U^2}{R}a_m\left.\right]\left[1 - \frac{(m+1)^2}{(2m+1)(2m+3)} + \frac{m^2}{(2m-1)(2m+1)}\right.$$

$$- \frac{(m+1)^2(m+2)}{(2m+1)(2m+3)} - \frac{m(m-1)^2}{(2m+1)(2m-1)}\right] + \frac{3}{2}\left[2Ua_{m-1}\frac{m-1}{2m-1}\frac{\dot{R}}{R} + U\dot{a}_{m-1} + \frac{1}{3}\frac{m}{2m-1}\dot{U}a_{m-1}\right]$$

$$+ \frac{9}{4}\frac{U^2}{R}\frac{(m-2)(m-1)m}{(2m-3)(2m-1)}a_{m-2}\left.\right\}P_m. \quad (4)$$

For the derivation of the governing equations for the bubble motion, size, and shape, the surface of a translating bubble is defined as the control surface. Since the pressure acts normally on the bubble surface, its direction forms an angle $(\theta - \beta)$ with the direction of bubble motion, where β is the angle between the normal vector $\mathbf{n}$ and the radial vector $\mathbf{r}_s$, as shown in Fig. 1. Then the force induced by the pressure can be written as

$$f = \int_A (-p)\cos(\theta - \beta)dA, \quad (5)$$

where A is the surface area of the bubble. The differential area on the bubble surface and $\cos(\theta - \beta)$ may be expressed in terms involving a_n's and the Legendre polynomials. The resulting expression of Eq. (6) is then integrated to yield

$$f = 2\pi R^2\rho\left(\frac{1}{3}R\dot{U} + \dot{R}U + \frac{1}{3}R\ddot{a}_1 + \dot{R}\dot{a}_1 + (8/3)\left[R\ddot{R} + \frac{3}{2}\dot{R}^2\right.\right.$$

$$+ (p_\infty/\rho) - \frac{2}{5}U^2\left](a_1/R) + \frac{1}{5}\left\{-3U\dot{a}_2 + [7\dot{U} + 13U(\dot{R}/R)](a_2/8)\right\} + (9/35)(U^2/R)a_3\right). \quad (6)$$

Now, according to Newton's second law, the equation of motion may be expressed as

$$f = m_g\dot{U} = \rho_{g0}\left(\frac{4}{3}\right)\pi R^3(0)\dot{U}, \quad (7)$$

where m_g is the mass of the gas inside the bubble, and ρ_{g0} is the initial density of the gas. By substituting Eqs. (6) into (7) to eliminate f, one obtains the expression for the motion of the bubble as

$$2\pi R^2\rho\{\frac{1}{3}R\dot{U} + \dot{R}U + \frac{1}{3}R\ddot{a}_1 + \dot{R}\dot{a}_1 + (8/3)(R\ddot{R} + \frac{3}{2}\dot{R}^2 + p_\infty/\rho - \frac{2}{5}U^2)a_1/R$$

$$+ \frac{1}{5}[-3U\dot{a}_2 + (7\dot{U} + 13U\dot{R}/R)a_2/8] + (9/35)(U^2/R)a_3\} = \rho_{g0}4\pi\dot{U}R^3(0)/3. \quad (8)$$

The force balance on the differential element of the bubble surface leads to the expression

$$\sigma(1/R_1 + 1/R_2) = p_{in} - p(r_s), \quad (9)$$

[8] P. M. Morse, and H. Feshbach, *Methods of Theoretical Physics* (McGraw-Hill Book Co., New York, 1953), Chap. 10, p. 1326.

FIG. 2. The time history of the translatory velocity and unperturbed radius of an initially nonspherical bubble moving in a quiescent liquid for $U(0) = 0.7$, $R(0) = 1$, $\dot{R}(0) = 0$, $P_\infty(0) = 7030$, and $P_\infty = 195$.
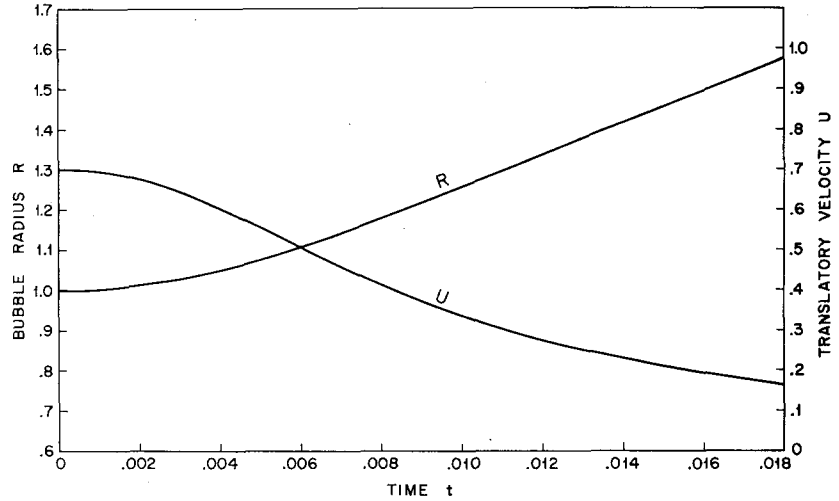
where σ is the surface tension, R_1 and R_2 are the principal radii of curvature of the bubble surface, and p_{in} and $p(r_s)$ are the pressures exerted upon the inside and outside surfaces of the bubble, respectively. It is assumed that the gas pressure inside the bubble is uniformly distributed, and the gas is ideal and undergoes a reversible polytropic process during the growth or collapse of the bubble. The sum of the curvatures up to the first-order correction may be obtained from Eq. (1) for a perturbed bubble. By substituting Eq. (4) together with the expression for a reversible polytropic process into Eq. (9) followed by equating all the coefficients of the P_n terms to zero, the equations for R and a_n are obtained:

Coefficient of P_0:

$$R\ddot{R}+\tfrac{3}{2}\dot{R}^2+(p_\infty-p_{in})/\rho-\tfrac{1}{4}U^2+2\sigma/R-\tfrac{1}{2}U\dot{a}_1-(U\dot{R}/R+\dot{U}/3)a_1=0. \tag{10}$$

Coefficients of P_1:

$$R\ddot{a}_1/2+3\dot{R}\dot{a}_1/2-(9/10)U^2a_1/R-(3/10)[3U\dot{a}_2+(\dot{U}+4U\dot{R}/R)a_2]+(27/70)U^2a_3/R+3\dot{R}U/2+R\dot{U}/2=0. \tag{11a}$$

Coefficients of P_2:

$$R\ddot{a}_2/3+\dot{R}\dot{a}_2+(-\ddot{R}/3-(54/35)U^2/R+4\sigma/\rho R^2)a_2+3U\dot{a}_1/2$$
$$+(\dot{U}/3+U\dot{R}/R)a_1-(3/14)[5U\dot{a}_3+(4\dot{U}+6U\dot{R}/R)a_3]+U^2a_4/R+3U^2/4=0. \tag{11b}$$

Coefficient of P_n for $n\geq 3$:

$$[R/(n+1)]\ddot{a}_n+[3/(n+1)]\dot{R}\dot{a}_n-[(n-1)/(n+1)]\ddot{R}a_n+(9/4)(U^2/R)a_n[1-(n+1)^2(n+3)/(2n+1)(2n+3)$$
$$+n(n^2-3n+1)/(2n-1)(2n+1)]+[(n-1)(n+2)/\rho R^2]\sigma a_n$$
$$+(9/4)[n(n+1)(n+2)/(2n+3)(2n+5)](U^2/R)a_{n+2}-[3/2(2n+3)][\tfrac{1}{3}(5n+2)\dot{U}-2(n+1)^2U\dot{R}/R]a_{n+1}$$
$$-[3(n+1)/2(2n+3)]U\dot{a}_{n+1}+\tfrac{3}{2}\{[2(n-1)/2n-1](U\dot{R}/R)a_{n-1}+U\dot{a}_{n-1}+[n/3(2n-1)]\dot{U}a_{n-1}\}$$
$$+[9(n-2)(n-1)n/4(2n-3)(2n-1)](U^2/R)a_{n-2}=0. \tag{11c}$$

Equation (10) is the bubble dynamics equation that must be solved simultaneously with Eq. (11).

RESULTS AND DISCUSSION

All equations derived in the previous Section may be made dimensionless by dividing the quantities of length, velocity, acceleration, time, and pressure by $R(0)$, $[\sigma/\rho R(0)]^{1/2}$, $\sigma/\rho[R(0)]^2$, $\{\rho[R(0)]^3/\sigma\}^{1/2}$, and $\sigma/R(0)$, respectively, where $R(0)$ is the initial radius of the bubble. The introduction of these dimensionless quantities does not cause any change in the form of those equations except that ρ and σ now drop out from the expressions. $U/[\sigma/\rho R(0)]^{1/2}$, the dimensionless velocity, is actually the Weber number. In the following, we always refer to the equations and physical quantities in dimensionless form unless indicated otherwise.

Equations (8), (10), and (11) were numerically integrated by the Runge–Kutta method using an IBM 7090 digital computer. From the experimental study, it is disclosed that sufficiently accurate results may be obtained by retaining the first 12 a_n's in the computer
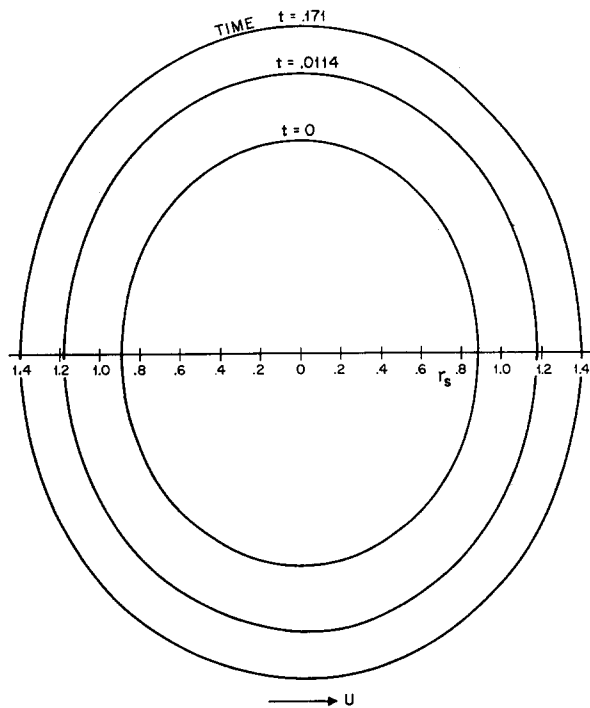
FIG. 3. The time history of the surface shape of an initially nonspherical bubble moving in a quiescent liquid for $U(0)=0.7$, $R(0)=1$, $\dot{R}(0)=0$, $P_\infty(0)=7030$ and $P_\infty=195$.

program. Therefore, together with equation (8), a total of fourteen simultaneous equations were solved for U, R and a_1 to a_{12}. The initial deformation of bubbles from the spherical shape as they travel with a constant velocity in a liquid may be calculated from the steady-state terms of Eqs. (10) and (11). The initial equilibrium pressure of gas within the bubble $p_{in}(0)$ can be evaluated from Eq. (10) which yields

$$p_{in}(0) = p_\infty(0) - U^2/4 + 2/R.$$

Numerical calculations were performed for a gas bubble moving with a constant velocity $U(0)=0.7$ in the quiescent water at 77°F (water density=0.997 g/cm³, surface tension for water–air system=71.97 dyn/cm). In general, $U(0)$ has to be selected so that the a_n's are within the validity of the perturbation technique. For the present case, $U(0)$ or equivalently the Weber number is less than 1.23, the stability criterion for a bubble in steady translatory motion.[5] The initial conditions correspond to $x(0)=0$, $R(0)=1$, $\dot{R}(0)=0$, $a_2(0)=0114031$, $a_4(0)=0.004934$, $a_6(0)=-0.000167$ and $a_n(0)=0$ for $n=1, 3, 5, 7$–12. Then a sudden change in the system pressure was imposed on the system, either a step increase from $p_\infty(0)=195$ or 3515 to $p_\infty=7030$ ($p_\infty=7030$ corresponds to one atmospheric pressure, $p_\infty=195$, corresponds to vapor pressure), or a step decrease from $p_\infty(0)=7030$ to $p_\infty=195$. $\gamma=1$ case, corresponding to an isothermal process of gas inside the bubble, is considered. Results are presented graphically in Figs. 2–6.

Figures 2 and 3 show the history of the translatory velocity, size and shape of the bubble for the case in which the system pressure undergoes a step change from $p_\infty(0)=7030$ to $p_\infty=195$. It is seen from these Figures that as the bubble grows, its translatory motion is slowed down, while its shape remains almost unchanged.

Figures 4 and 5 are the results for the case where the system pressure undergoes a step change from $p_\infty(0)=195$ to $p_\infty(0)=7030$. Figure 4 shows that as the collapse is accelerated, the translatory velocity increases abruptly. In the course of collapsing, the bubble shape gradually becomes more and more spherical. However, in the later stage of collapse, the translatory acceleration and rate of the collapse of the bubble become large. Consequently, a_n's begin to increase and finally become very large abruptly. This indicates the threshold of instability in bubble shape. As shown in Fig. 5, an indentation is seen on the bubble surface. Its location depends upon $U(0)$ and the change in the system
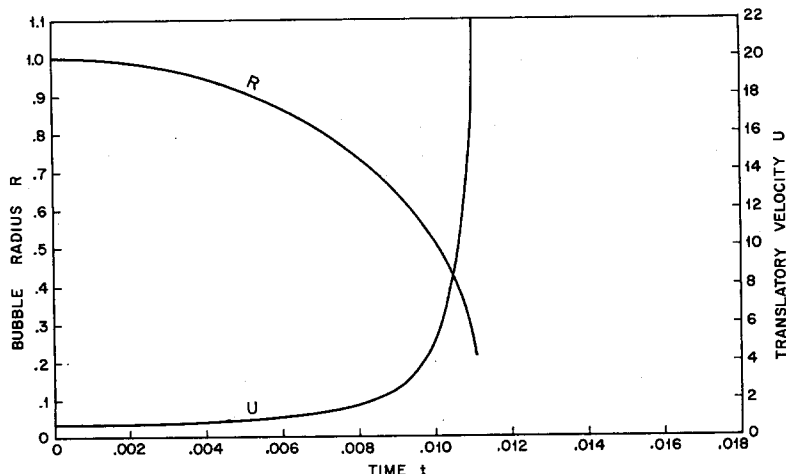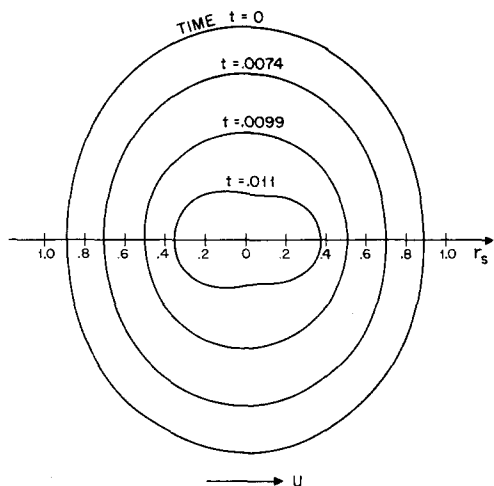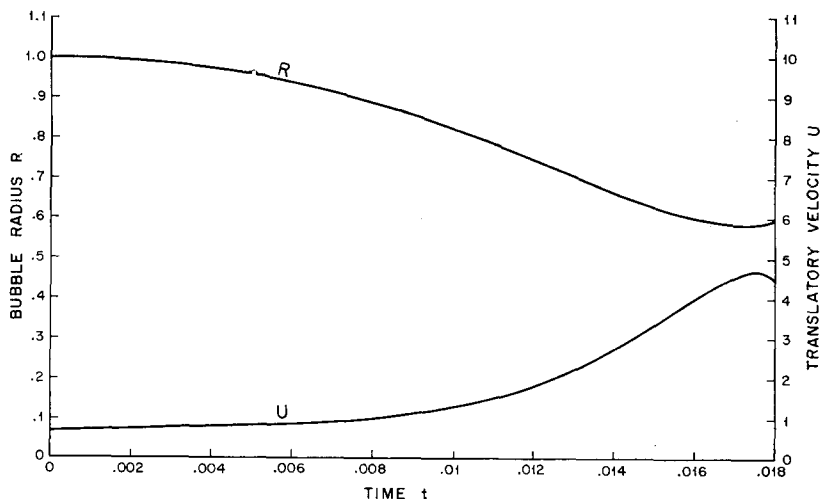

FIG. 4. The time history of the translatory velocity and unperturbed radius of an initially nonspherical bubble moving in a quiescent liquid for $U(0)=0.7$, $R(0)=1$, $\dot{R}(0)=0$, $P_\infty(0)=195$, and $P_\infty=7030$.

FIG. 5. The time history of the surface shape of an initially nonspherical bubble moving in a quiescent liquid for $U(0) = 0.7$, $R(0) = 1$, $\dot{R}(0) = 0$, $P_\infty(0) = 195$, and $P_\infty = 7030$.

and

$$\ddot{R} = U^2/4R - \tfrac{3}{2}\dot{R}^2/R + (p_{in} - p_\infty)/R - 2/R^2 \qquad (13)$$

obtained from Eqs. (8) and (10), respectively, by neglecting the a_n's.

Equation (12) indicates that its translatory motion is decelerated as a bubble grows and *vice versa*. This explains the U–R relationship illustrated in Figs. 2 and 4. When Eq. (12) is integrated, it yields

$$U = U(0)[R(0)/R]^3. \qquad (14)$$

Equation (13) shows that the acceleration of the bubble surface displacement is induced by the forces due to $U^2/4R$, $-\tfrac{3}{2}\dot{R}^2/R$, $(p_{in} - p_\infty)/R$, and $-2/R^2$. In the initial stage of bubble collapse shown in Fig. 6, the negative pressure force $(p_{in} - p_\infty)/R$ is a dominating factor: but as the bubble travels down stream, Eq. (12) indicates that its translatory motion is further accelerated as the collapse continues. It can be seen from Eq. (14) that for an isothermal process, the gas pressure inside the bubble p_{in} is linearly proportional to the translatory velocity U. Hence, as the translatory bubble is accelerated following the bubble collapse, the absolute magnitude of the dominating term $(p_{in} - p_\infty)/R$ decreases. Eventually, the right-hand side of Eq. (13) becomes zero and then changes to positive; and consequently, the collapse rate is slowed down to zero followed by rebound. As the bubble starts to rebound, the right side of Eq. (12) changes from a positive quantity to a negative one, indicating the deceleration of the bubble motion.

pressure. Figure 6 shows the time history of the translatory velocity and size of the bubble for the case where the system pressure undergoes a step change from $p_\infty(0) = 3515$ to $p_\infty = 7030$. It is interesting to note that the translatory velocity increases to a maximum as the collapse rate approaches zero and the bubble starts to rebound. During the course of the collapse, the bubble shape becomes more and more spherical followed by indentation in the direction normal to its translating motion. It is our expectation that after the bubble rebounds and grows to a maximum size, it will follow a collapsing course again.

The mechanism related to the change in the bubble velocity and the rate of growth or collapse may be disclosed from the equations

$$\ddot{x}(=\dot{U}) = -3U\dot{R}/R \qquad (12)$$

CONCLUSION

When a gas bubble is in translatory motion in a liquid following a sudden change in the system pressure, the bubble may be accelerated or decelerated as the

FIG. 6. The time history of the translatory velocity and radius of an initially nonspherical bubble moving in a quiescent liquid for $U(0) = 0.7$ $R(0) = 1$, $\dot{R}(0) = 0$, $P_\infty(0) = 3515$, and $P_\infty = 7030$.

result of the interaction between the translatory velocity and the rate of growth or collapse. In general, a moving bubble grows and maintains a stable surface shape when the liquid is subjected to a step decrease in pressure. However, if the pressure change is a step increase, then under certain conditions dependent upon

the initial conditions and $p_\infty - p_\infty(0)$, a bubble may collapse and rebound. During the process of collapse, the bubble shape becomes spherical in the earlier period of time, and then becomes irregular as the rate of collapse and translatory acceleration of the bubble increases.

Pressure and Temperature Dependence of the Acoustic Velocities in Polymethylmethacrylate

JAMES R. ASAY,* DONALD L. LAMBERSON, AND ARTHUR H. GUENTHER

Air Force Weapons Laboratory, Kirtland AFB, Albuquerque. New Mexico 87117

(Received 26 August 1968)

The acoustic velocities in polymethylmethacrylate have been measured with an ultrasonic pulse-echo technique as functions of frequency, temperature, and pressure. At atmospheric pressure, data on the velocities and attenuation coefficients were obtained for the temperature range of 22°-75°C in the frequency range of 6-30 MHz. For the measurements of velocity and attenuation as a function of frequency, the complex adiabatic bulk modulus was calculated at room temperature and atmospheric pressure for the above frequencies. At temperatures of 25°, 40°, 55°, and 75°C, the pressure dependence of the longitudinal and shear velocity was determined to 150 kpsi at a frequency of 6 MHz. It was found that the measured velocities under increasing pressure conditions were generally lower than those of decreasing pressure by about 0.5% for the longitudinal measurements and about 1% for the shear measurements. However, measurements of the velocities at atmospheric pressure after the specimens had been exposed to 150 kpsi were usually within 0.1% of the initial values. A discussion is presented which compares the continuity of the present data with equation of state determinations in PMMA at elevated pressures.

INTRODUCTION

The high-pressure equation of state of solids, as determined through ultrasonic techniques, has received considerable interest in recent years, primarily because of the accuracy with which acoustic velocities can be determined. In principle, the determination of the pressure and temperature dependence of the acoustic velocities in elastic solids allows a direct determination of the PVT surface over the ranges for which the data are obtained. Anderson[1] has significantly extended this technique by showing how the pressure dependence of the velocities can be used to define the quantities appearing in a semiempirical equation of state initially proposed by Murnaghan.[2] Providing the material does not exhibit phase changes over the region of interest, Anderson shows that the Murnaghan equation thus obtained can be used to estimate the pressure-volume relation to pressures one or two orders of magnitude higher than the range over which the ultrasonic data were obtained. This approach has been applied to a

number of materials,[1,3] with the remarkable result that the equation of state as estimated from ultrasonic pressure measurements over the range of about 3-10 kbars typically agrees to within a few percent of the equation of state as obtained by standard compressibility techniques to ~100 kbars or dynamic evaluations to greater than 1000 kbars.

This method has not previously been applied to polymeric materials, mainly because of the scarcity of accurate pressure measurements of the acoustic velocities in plastics. In addition, polymers generally exhibit frequency dependent elastic moduli[4] and volume creep under hydrostatic pressure,[5] so that the volume is a function of time as well as pressure.

Another problem specifically dealing with plastics is that the elastic moduli generally are not linear functions of either pressure or temperature. This complicates the definition of an equation of state, since,

* Submitted in partial fulfillment for the degree of Master of Science at the University of New Mexico.

[1] O. L. Anderson, J. Phys. Chem. Solids **27**, 547 (1966).

[2] F. D. Murnaghan, *Finite Deformations of an Elastic Solid* (John Wiley & Sons, Inc., New York, 1951).

[3] J. R. Asay, S. R. Urzendowski, and A. H. Guenther, *Ultrasonic and Thermal Studies of Selected Plastics, Laminated Materials and Metals* (Tech. Rept. No. AFWL-TR-67-91, Kirtland AFB, New Mexico, 1968).

[4] R. S. Marvin and J. E. McKinney, *Physical Acoustics* (Academic Press, Inc., New York, 1965), Vol. II, Pt. B, Chap. 9.

[5] W. N. Findley, R. M. Reed, and P. Stern, J. Appl. Mech. **34**, 895 (1967).